



## Article

# Study on the Differences between the Extraction Results of the Structural Parameters of Individual Trees for Different Tree Species Based on UAV LiDAR and High-Resolution RGB Images

Haotian You <sup>1,2</sup>, Xu Tang <sup>1</sup>, Qixu You <sup>1</sup>, Yao Liu <sup>1</sup>, Jianjun Chen <sup>1</sup> and Feng Wang <sup>1,\*</sup>

<sup>1</sup> College of Geomatics and Geoinformation, Guilin University of Technology, No. 12 Jian'gan Road, Guilin 541006, China; youht@glut.edu.cn (H.Y.); 2120211898@glut.edu.cn (X.T.); 2120211909@glut.edu.cn (Q.Y.); 1020211833@glut.edu.cn (Y.L.); chenjj@glut.edu.cn (J.C.)

<sup>2</sup> Guangxi Key Laboratory of Spatial Information and Geomatics, Guilin University of Technology, No. 12 Jian'gan Road, Guilin 541004, China

\* Correspondence: wangfeng92@glut.edu.cn

**Abstract:** Light Detection and Ranging (LiDAR) points and high-resolution RGB image-derived points have been successfully used to extract tree structural parameters. However, the differences in extracting individual tree structural parameters among different tree species have not been systematically studied. In this study, LiDAR data and images were collected using unmanned aerial vehicles (UAVs) to explore the differences in digital elevation model (DEM) and digital surface models (DSM) generation and tree structural parameter extraction for different tree species. It was found that the DEMs generated based on both forms of data, LiDAR and image, exhibited high correlations with the field-measured elevation, with an  $R^2$  of 0.97 and 0.95, and an RMSE of 0.24 and 0.28 m, respectively. In addition, the differences between the DSMs are small in non-vegetation areas, whereas the differences are relatively large in vegetation areas. The extraction results of individual tree crown width and height based on two kinds of data are similar when all tree species are considered. However, for different tree species, the *Cinnamomum camphora* exhibits the greatest accuracy in terms of crown width extraction, with an  $R^2$  of 0.94 and 0.90, and an RMSE of 0.77 and 0.70 m for LiDAR and image points, respectively. In comparison, for tree height extraction, the *Magnolia grandiflora* exhibits the highest accuracy, with an  $R^2$  of 0.89 and 0.90, and an RMSE of 0.57 and 0.55 m for LiDAR and image points, respectively. The results indicate that both LiDAR and image points can generate an accurate DEM and DSM. The differences in the DEMs and DSMs between the two data types are relatively large in vegetation areas, while they are small in non-vegetation areas. There are significant differences in the extraction results of tree height and crown width between the two data sets among different tree species. The results will provide technical guidance for low-cost forest resource investigation and monitoring.

**Keywords:** UAV LiDAR; high-resolution RGB images; DEM; DSM; individual tree structural parameters; different tree species



**Citation:** You, H.; Tang, X.; You, Q.; Liu, Y.; Chen, J.; Wang, F. Study on the Differences between the Extraction Results of the Structural Parameters of Individual Trees for Different Tree Species Based on UAV LiDAR and High-Resolution RGB Images. *Drones* **2023**, *7*, 317. <https://doi.org/10.3390/drones7050317>

Academic Editor: Diego González-Aguilera

Received: 8 March 2023

Revised: 27 April 2023

Accepted: 8 May 2023

Published: 10 May 2023



**Copyright:** © 2023 by the authors. Licensee MDPI, Basel, Switzerland. This article is an open access article distributed under the terms and conditions of the Creative Commons Attribution (CC BY) license (<https://creativecommons.org/licenses/by/4.0/>).

## 1. Introduction

As the world's largest terrestrial ecosystem, forests are not only an important part of the global carbon cycle, but also the main driving force of global climate change and the main component of biodiversity [1]. Moreover, individual trees serve as the basic unit of forest ecosystems and play a crucial role in forest resource quantification research, as well as being an important input variable for various studies, such as on carbon storage, climate change, and biodiversity. Therefore, it is particularly important to accurately obtain the structural parameters of individual trees.

Field measurements can accurately obtain individual tree structural parameters, but they are usually time-consuming and laborious, and the data update frequency is relatively long. Light Detection and Ranging (LiDAR) is a technique that uses a laser transmitter to send a laser beam and obtain three-dimensional information on ground and object surfaces by receiving the reflected signal from these surfaces. Therefore, it can penetrate the forest canopy and obtain vertical and horizontal structural information, which compensates for the shortcomings of field measurements and can replace them in some cases. It has been widely used for forest individual tree structural parameter extraction, achieving good results [2–5]. For instance, Jaakkola et al. [6] estimated individual tree heights using the LiDAR data from unmanned aerial vehicles (UAVs), and the RMSE was 0.30 cm. da Cunha Neto et al. [7] extracted the height of individual trees based on UAV LiDAR data, and the  $R^2$  was 0.73. The commonly used LiDAR data at present mainly include spaceborne LiDAR, terrestrial LiDAR, airborne LiDAR, and UAV LiDAR. Due to the coarse resolution, spaceborne LiDAR data are widely used in the estimation of forest structural parameters at the sample scale. Although terrestrial LiDAR can accurately estimate the diameter of the breast height of an individual tree, it is difficult to accurately extract the height and crown width owing to the difficulty in obtaining data from the upper layer of the forest canopy. Because of the high cost, the density of airborne LiDAR data is relatively low, which has a certain effect on the extraction of individual tree structural parameters. UAV LiDAR is advantageous, as it is flexible to operate and is low cost. Therefore, it can obtain high-density data with a low flight altitude and multiple flights, making it the most used form of LiDAR data for extracting individual tree structural parameters at present.

In addition to using UAV LiDAR to directly obtain three-dimensional point cloud data, it is also possible to generate such data through processing high-resolution RGB stereo images. The development of structure from motion (SfM) and multi-view stereo (MVS) technologies has made it possible to rapidly extract three-dimensional point cloud data using high-resolution stereo images [8,9]. In comparison to LiDAR data, this method greatly reduces the cost of data acquisition. Therefore, it has been widely used to extract individual tree structural parameters [10,11]. For example, Karpina et al. [12] extracted the heights of 22 Scottish pines on a plantation using point data derived from UAV high-resolution images, with an average accuracy of 5 cm. Guerra-Hernández et al. [13] estimated the growth changes in a pine plantation from 2015 to 2017 using point data derived from multi-temporal UAV images. The results showed that the growth in tree height and biomass were  $0.45 \text{ m} \pm 0.12 \text{ m}$  and  $198.7 \pm 93.9 \text{ kg}$ , respectively. Tang et al. [14] measured the monthly growth in individual tree height based on point data derived from multi-temporal UAV images. Dempewolf et al. [15] measured the height growth of different tree species during a growing season based on point data derived from multi-temporal UAV images.

To assess the advantages and disadvantages of extracting individual tree structural parameters using point data generated from LiDAR and high-resolution images, researchers have conducted extensive related research. For instance, Guerra-Hernández et al. [16] utilized point data generated from UAV LiDAR and images to determine the average tree height of a eucalyptus plantation. The results showed that the extracted tree heights from the point data were almost identical, with a RMSE of 2.80 and 2.84 m, respectively. Wallace et al. [17] also utilized the above two data types to estimate tree height, and the RMSEs were 0.92 and 1.30 m, respectively. Guerra-Hernández et al. [18] estimated individual tree volume in a eucalyptus plantation using both UAV LiDAR and images, with a RMSE of 0.026 and  $0.030 \text{ m}^3$ , respectively. These results indicate that the difference in the results of the extraction of individual tree structural parameters, such as tree height and volume, between LiDAR and high-resolution imagery-derived point data is small when tree species are not considered. However, different tree species usually exhibit certain differences in their horizontal and vertical structures during growth; thus, the growth differences between tree species may lead to differences in the extraction results of individual tree structural parameters based on two-point data. In addition, the principles of obtaining point data for LiDAR and images are different. Specifically, LiDAR obtains 3D points through obtaining

laser pulse echoes, while image points are generated based on stereo images using the SFM algorithm. Thus, LiDAR data can penetrate the forest canopy and obtain more points inside the canopy and ground points, while the images may encounter blind areas caused by the canopy, with the generated points consisting of more canopy surface points and few ground points under the canopy. Therefore, there may also be some differences in generating digital elevation models (DEMs) and digital surface model (DSMs) between the two-point data in different areas, such as bare land, grassland, and forest. Therefore, it is necessary to study the differences in DEM and DSM generation results in different regions and the differences in individual tree structural parameter extraction results of different tree species based on the two-point data.

Accordingly, this study utilized a UAV to collect LiDAR data and stereo images, and DEMs, DSMs, and CHMs in different regions were generated through data processing. Then, individual tree heights and crown widths of four different tree species were extracted based on the individual tree segmentation results of the CHM. Furthermore, comparative research was conducted to systematically explore the differences in DEMs and DSMs in different regions and the differences in the individual tree structural parameter extraction results of different tree species based on LiDAR points and image points. The study aims to achieve the following objectives: (1) to explore the differences in generating DEMs and DSMs in different regions from LiDAR points versus image points; (2) to explore the differences in the extraction results of individual tree heights and crown widths from LiDAR points versus image points; and (3) to explore the differences in extracting individual tree heights and crown widths of different tree species from LiDAR points versus image points. The results of this study not only provide technical guidance for low-cost forest resource investigation and monitoring, but also provide scientific data support for the sustainable management and development of forest resources.

## 2. Materials and Methods

### 2.1. Study Area

As shown in Figure 1, The study was carried out in a mixed broad-leaved tree plantation, with an area of 2 hectares in Guilin, Guangxi Zhuang Autonomous Region, China ( $110^{\circ}17'44''$  E– $110^{\circ}17'50''$  E,  $25^{\circ}3'46''$  N– $25^{\circ}3'50''$  N). The terrain in most parts was relatively flat, with only some steep slopes in the southern and southeastern regions. The predominant tree species mainly included *Cinnamomum camphora* (*Cinnamomum camphora* (L.) Presl), *Osmanthus fragrans* (*Osmanthus* sp.), *Liriodendron chinense* (*Liriodendron chinense* (Hemsl.) Sarg.), and *Magnolia grandiflora* (*Magnolia grandiflora* L.). Among the four tree species, *Cinnamomum camphora*, *Osmanthus fragrans*, and *Magnolia grandiflora* are evergreen broad-leaved trees, whereas *Liriodendron chinense* is a deciduous broad-leaved tree.

### 2.2. Data Collection and Processing

#### 1. Field Data

On 6 October 2021, a total station was employed in conjunction with real-time kinematic (RTK) measurements to obtain the horizontal positioning and the elevation information for individual trees. In addition, 21 ground points in the open areas free of canopy cover were collected using RTK on 1 April 2023. The tree heights were measured with a measuring pole while recording the species information. The crown diameters of individual trees were measured in both the east–west and north–south directions determined via a mobile phone compass. The edges of individual tree crowns were visually determined by people standing under the canopy. The mean of the crown diameter measurements in the east–west and north–south directions is used as the crown width. A total of 143 trees were measured, including 8 *Cinnamomum camphora*, 87 *Osmanthus fragrans*, 14 *Liriodendron chinense*, and 34 *Magnolia grandiflora*. The specific statistical results are shown in Table 1.

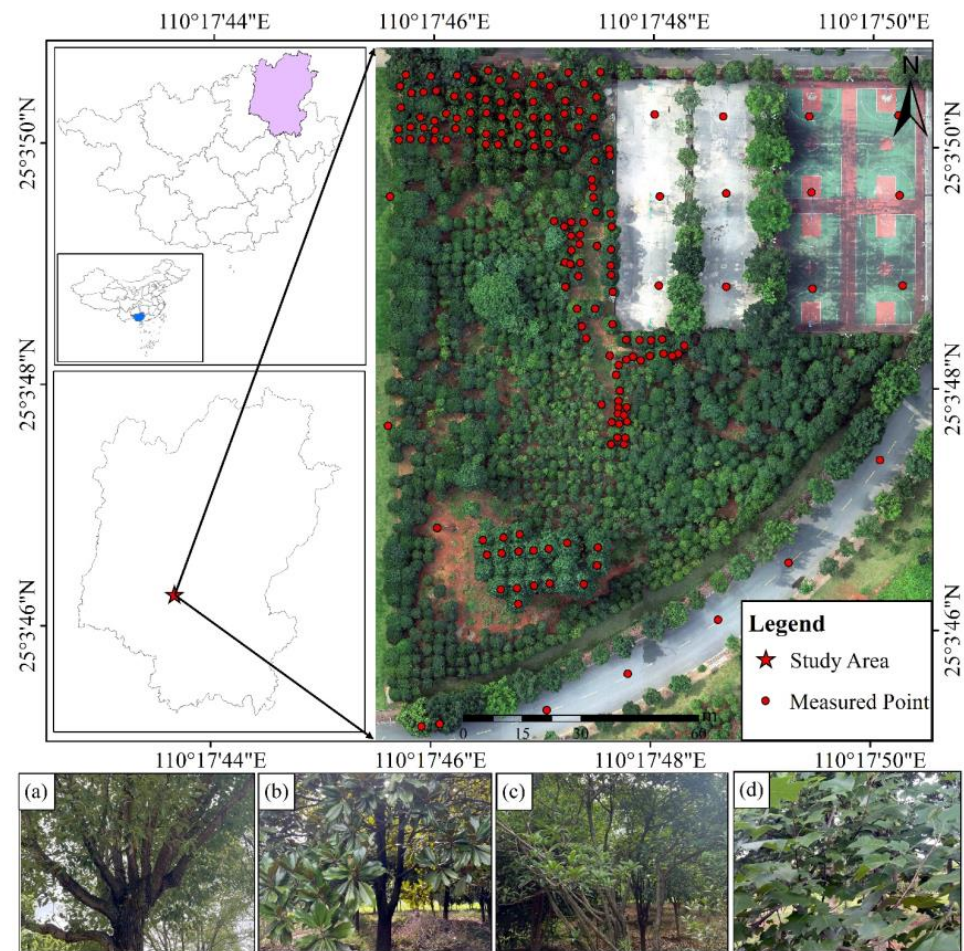


**Figure 1.** Location of the study area: (a) *Cinnamomum camphora*; (b) *Magnolia grandiflora*; (c) *Osmanthus fragrans*; (d) *Liriodendron chinense*.

**Table 1.** Statistical results of field measurement (SD represents standard deviation).

Trees Species	Number (Tree)	Mean Tree Height (m)	Mean Crown Width (m)	SD of Tree Height (m)	SD of Crown Width (m)
<i>Cinnamomum camphora</i>	8	8.83	6.99	0.75	1.03
<i>Osmanthus fragrans</i>	87	4.19	3.63	0.76	0.87
<i>Liriodendron chinense</i>	14	16.16	6.06	0.68	1.25
<i>Magnolia grandiflora</i>	34	8.32	4.88	0.86	0.75

## 2. UAV LiDAR Point Cloud Data

On 4 July 2022, the LiDAR points cloud data (hereinafter referred to as LiDAR points) were obtained using a DJI Zenmuse L1 sensor mounted on a DJI Matrice 300 RTK UAV. The operation mode of the UAV was mapping aerial photography, with a flight altitude of 80 m and a side overlap of 70%. The echo mode was dual echoes, with a scanning frequency of 240 KHZ and a scanning mode of repeated scanning.

The acquired LiDAR data were preprocessed to generate LiDAR points in LAS format using DJI Terra V3.6.8 software; the average point density of LiDAR points was 439.75 points/m<sup>2</sup>. The LiDAR points were denoised and classified, and then the classified ground points were interpolated into a DEM using the inverse distance weighting interpolation algorithm in LiDAR360 V6.0 software. The inverse distance weighting interpolation algorithm is a distance-based interpolation method that assumes that similar points in space have similar attribute values. The algorithm uses the reciprocal of distance as the weight,

so that the weight of points closer to each other is larger, while the weight of points farther away is smaller, enabling a more accurate estimation of the elevation values of unknown points. To avoid the effect of pits in the CHM for individual tree segmentation, the pit-free algorithm was used to generate a DSM using “lidR” packages in R 4.2.1 software [19]. Specifically, the classified non-ground points were normalized based on the DEM. The normalized points were separated into multiple layers with different height thresholds and every layer was interpolated into the DSM using the triangular irregular network (TIN) algorithm. The DSMs of all layers were stacked to generate the final DSM using the maximum value. A CHM with a spatial resolution of 2 cm could be obtained by subtracting the DEM from the DSM. Through multiple experiments, it was found that the generated CHM could effectively remove the pits by using height thresholds of 0, 1, 5, 8, and 10 m.

### 3. High-resolution RGB Stereo Image-derived Point Cloud Data

On 4 July 2022, high-resolution RGB stereo images were obtained using a consumer-grade RGB camera mounted on a DJI Phantom 4 RTK UAV. The flight mode was a five-directional flight mode, with a flight altitude of 60 m. The longitudinal overlap was 80%, and the side overlap was 70%.

The acquired high-resolution RGB stereo images were processed to generate a DSM using ContextCapture 4.4.12 software and simultaneously were processed to generate point data (hereinafter referred to as image points) using Pix4D 4.7.5 software. The average point density of image points was  $1015.68/\text{m}^2$ . Then, the image points were denoised and classified, and then the classified ground points were interpolated into the DEM using the inverse distance weighting interpolation method algorithm in LiDAR360 V6.0 software [20]. A CHM with a spatial resolution of 2 cm was obtained by subtracting the DEM from the DSM.

The accuracy of the DEM is closely related to the subsequent generation of the CHM. Therefore, the differences between the DEMs generated from LiDAR and image points and field-measured elevation were evaluated using  $R^2$  and root mean square error (RMSE) [18,21].

#### 2.3. Individual Tree Crown Segmentation

The watershed segmentation algorithm is a segmentation method based on the mathematical morphology of topological theory. The basic idea is to treat the inverted CHM as a topographic terrain image, where the elevation of each point is indicated by its grayscale value. Each local minimum and its affected area are called catchment basins, and the point on the boundary between the catchment basins becomes the watershed [22]. The watershed algorithm involves an iterative calculation process, mainly including two steps: sorting and flooding. During the sorting process, the grayscale values of each pixel are sorted from low to high. Then, during the flooding process from low to high, a first-input–first-output (FIFO) structure is used to judge and label each minimum value in the image domain at a certain height. Due to the good response to weak edges, the watershed algorithm has been successfully used in individual tree segmentation research and has achieved good segmentation results [23–25]. Therefore, the watershed algorithm was used for individual tree segmentation in this study. During the individual tree segmentation process, it was necessary to determine the values of two parameters: the Gaussian smoothing factor and the smoothing window radius. Through multiple experiments with LiDAR360 V6.0 software, the Gaussian smoothing factor was set to 16, and the smoothing window radius was set to 111 pixels.

To further assess the accuracy of the individual tree segmentation results, a comparison was made between the results obtained from the watershed algorithm and the field-measured data. The accuracy of individual tree segmentation results was evaluated using recall (r), precision (p), and F-score (F) [26,27].

#### 2.4. Individual Tree Structure Parameter Extraction

Based on the individual tree segmentation results, individual tree crown widths and heights were extracted. Specifically, the four corner points of each tree crown were calculated based on the vectorized individual tree segmentation results using ArcGIS 10.6 software. By subtracting the northernmost coordinates from the southernmost coordinates, and the easternmost coordinates from the westernmost coordinates of the four points on the tree crown, then taking the average, an individual tree crown width can be obtained. At the same time, the local maximum method was used in ArcGIS 10.6 software to extract the maximum CHM values within the vectorized region of each individual tree segmentation as the extraction results for the individual tree heights.

To further explore the differences in the extraction results of individual tree structural parameters between LiDAR points and image points for different tree species, the extraction results of individual tree crown widths and tree heights for different tree species were statistically analyzed and compared.

### 3. Results

#### 3.1. Analysis of the Generation Results of the DEMs and DSMs

##### 1. Results of the DEMs

The correlations between the DEMs generated from image points and LiDAR points and field-measured elevations were analyzed, as shown in Figure 2.

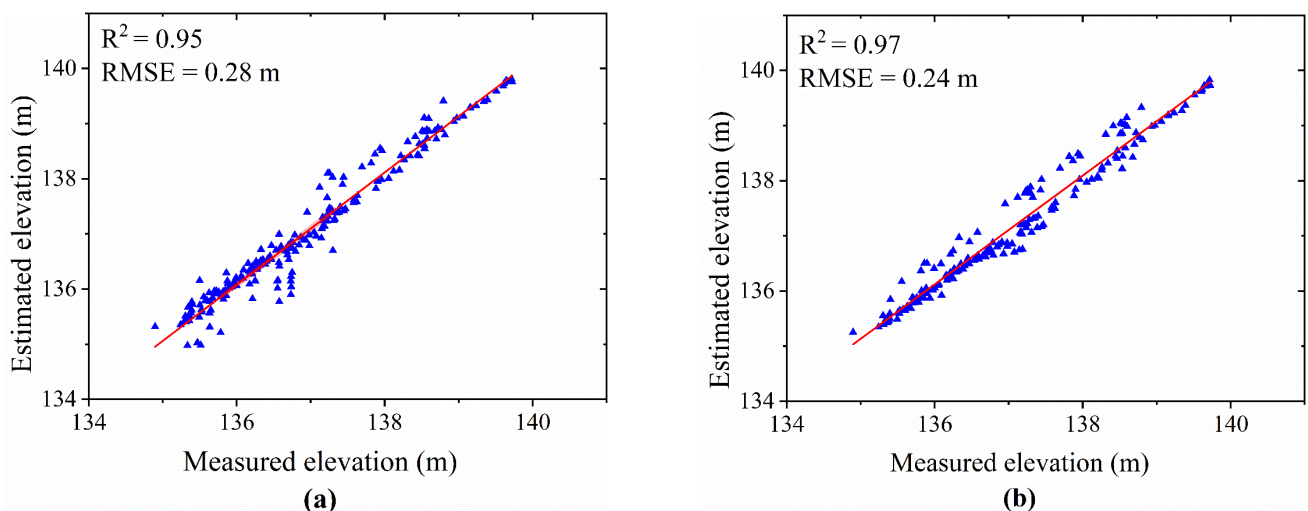


**Figure 2.** Elevation correlation analysis results: (a) comparing results of the DEMs generated from image points and field-measured elevation; (b) comparing results of the DEMs generated from LiDAR points and field-measured elevation.

The results shown in Figure 2 indicate that the DEMs generated from both image points and LiDAR points are highly correlated with field-measured elevations, with an  $R^2$  of 0.95 and 0.97, and a RMSE of 0.28 and 0.24 m, respectively. The difference in correlation results was evaluated through a *t*-test in Python, and the *p*-value was 0.76, which indicated that there was no significant difference between the DEMs generated based on the image points and the LiDAR points. The spatial distributions of the DEMs generated based on the image points and LiDAR points, as well as the differences, are shown in Figure 3.

The results in Figure 3a,b show that both DEMs' values are within the range of 134–140 m, but the DEM generated from LiDAR points exhibits smoother readings in areas with a high canopy closure. Additionally, the difference between two DEMs in areas with a high canopy closure is also relatively large, as shown in Figure 3c.

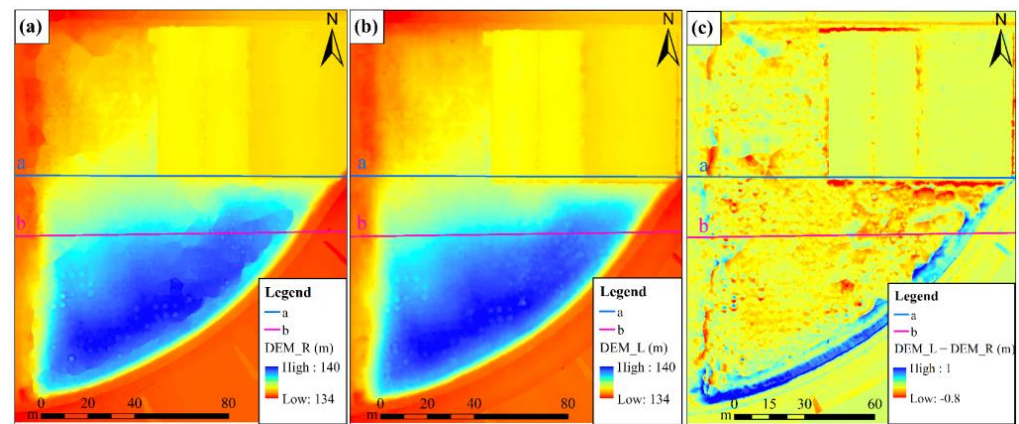


**Figure 3.** Spatial distribution of DEMs and the differences: (a) DEM generated based on image points; (b) DEM generated based on LiDAR points; (c) difference between the two DEMs.

To further demonstrate the differences between the two DEMs, two cross sections, a and b, with relatively high and low canopy closure, respectively, were selected on the spatial distributions of the DEMs (as shown in Figure 3) and are presented in Figure 4.

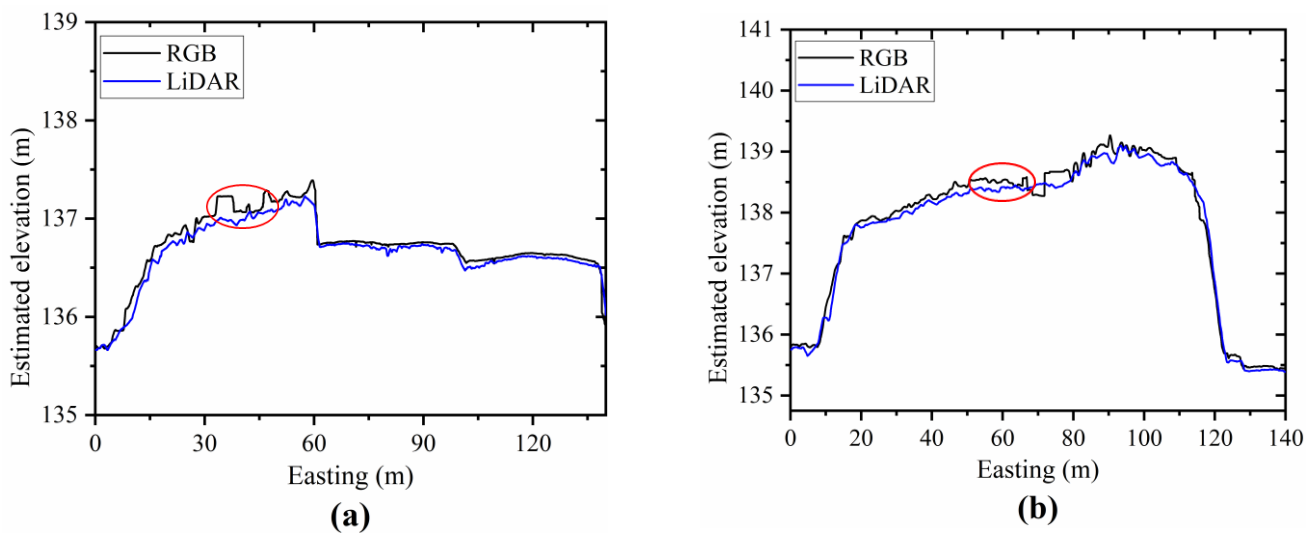


**Figure 4.** Distribution maps of elevation differences between the two DEMs for different cross sections: (a) cross section a; (b) cross section b.

According to Figure 4, it is evident that the elevation values of the DEMs generated based on image points are generally higher than those obtained from LiDAR points. In areas without forest, the elevation values of the two DEMs are almost identical. However, as the forest canopy closure increases, the differences between the values of the two DEMs tend to increase.

## 2. Results of the DSMs

Compared to ground points, both image points and LiDAR points include more forest canopy points, so the generated DSM has higher accuracy in theory. However, further verification is needed to explore the differences between the DSMs generated from LiDAR points and image points. The elevation distributions of the DSMs generated based on image points and LiDAR points, as well as the differences, are shown in Figure 5.

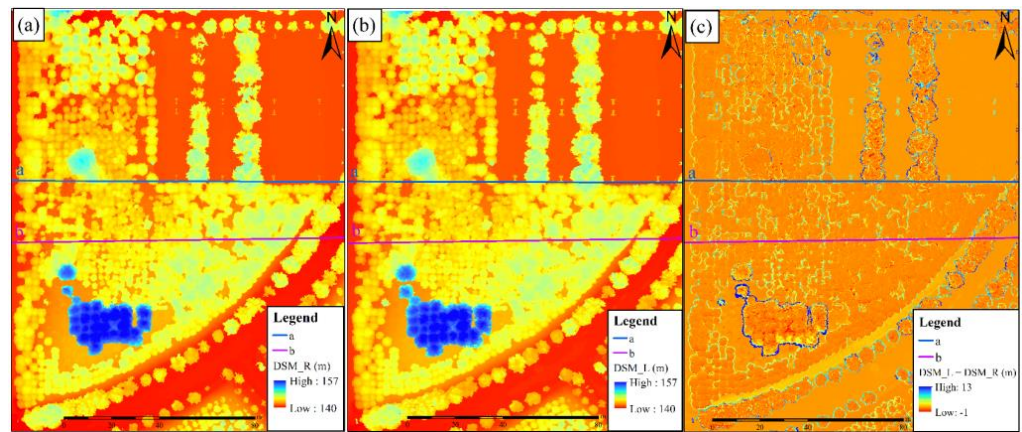


**Figure 5.** Spatial distribution of the DSMs and the differences: (a) DSM generated based on image points; (b) DSM generated based on LiDAR points; (c) difference between the two DSMs.

The results in Figure 5a,b show that both DSMs’ values are within the range of 140–157 m, indicating that the maximum tree height is within 15 m. As shown in Figure 5c, the differences between the DSMs mainly occur at the boundary of the tree canopy.

To further explore the differences between the DSMs, two cross sections, a and b, with relatively high and low canopy closure, respectively, were selected on the spatial distributions of the DSMs (as shown in Figure 5) and are presented in Figures 6 and 7.

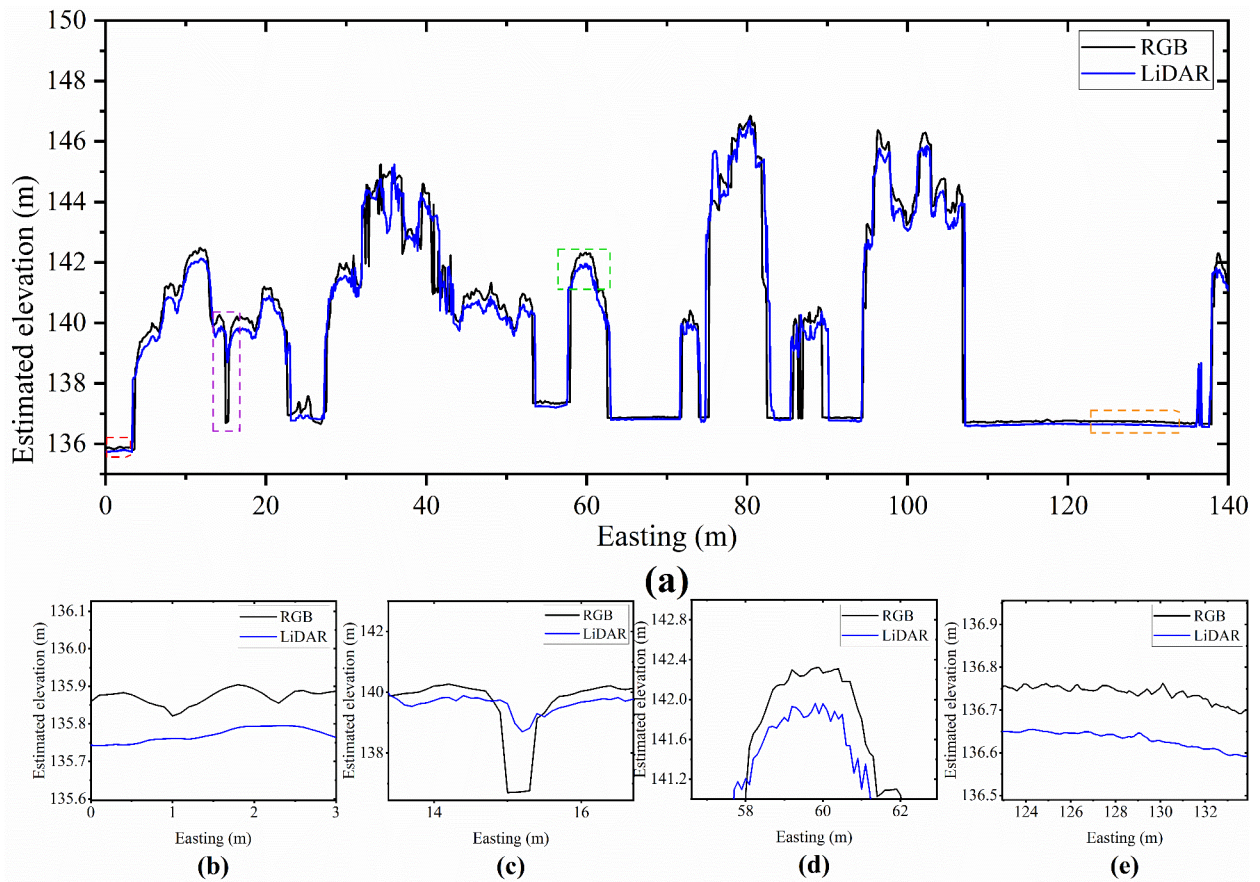


**Figure 6.** Cross section a: (a) elevation distribution map; (b) grassland; (c) canopy boundary; (d) canopy top; (e) flatland. (Note: The red, purple, green, and orange rectangles correspond to the grassland, canopy boundary, canopy top, and flatland, respectively).



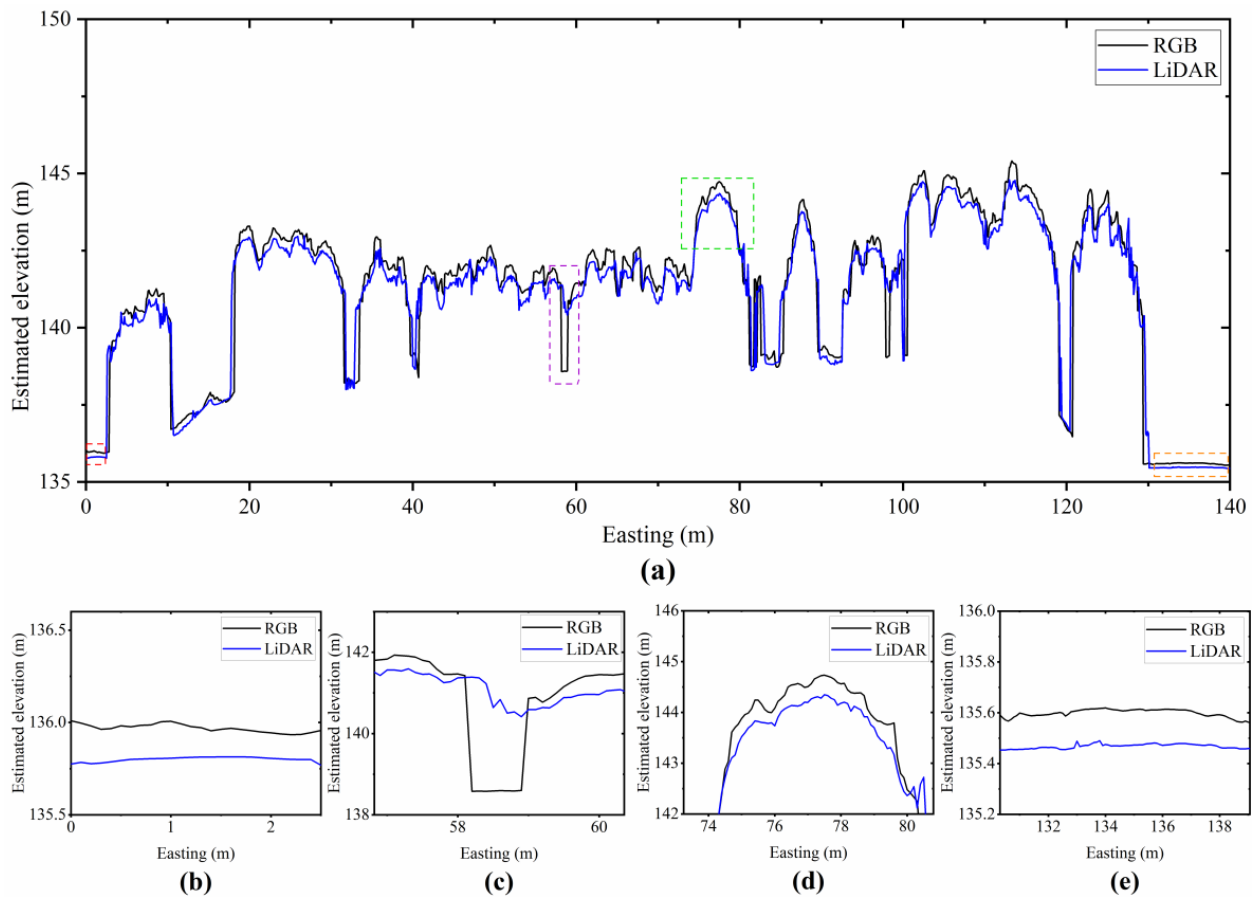


**Figure 7.** Cross section b: (a) elevation distribution map; (b) grassland; (c) canopy boundary; (d) canopy top; (e) flatland. (Note: The red, purple, green, and orange rectangles correspond to the grassland, canopy boundary, canopy top, and flatland, respectively).

Figures 6a and 7a indicate that the elevation values of the DSM generated based on image points are higher than those obtained from LiDAR points. Specifically, in the case of grassland areas, the elevation values of the DSM generated from image points are higher than those obtained from LiDAR points, as shown in Figures 6b and 7b. In the canopy boundary area, the DSM generated based on LiDAR points has higher elevation values than those obtained from image points, as shown in Figures 6c and 7c. However, for the canopy top, the elevation values of the DSM generated from image points are higher than those obtained from LiDAR points, as shown in Figures 6d and 7d. In the case of flatland areas, the elevation values of the DSM generated from image points are higher than those obtained from LiDAR points, but the differences are relatively small, only about 0.1 m, as shown in Figures 6e and 7e.

### 3.2. Analysis of Individual Tree Segmentation Results and Extraction Results for the Structural Parameters of Individual Trees

#### 1. Segmentation Results for Individual Trees

The segmentation results for individual trees based on the CHM using the watershed algorithm are shown in Figure 8.

As shown in Figure 8, accurate segmentation results were obtained using the watershed algorithm based on the CHMs generated from both image points and LiDAR points, but there are still some over-segmentations and under-segmentations. The segmentation results of 143 trees shown in Figure 8 were statistically analyzed, as shown in Table 2.

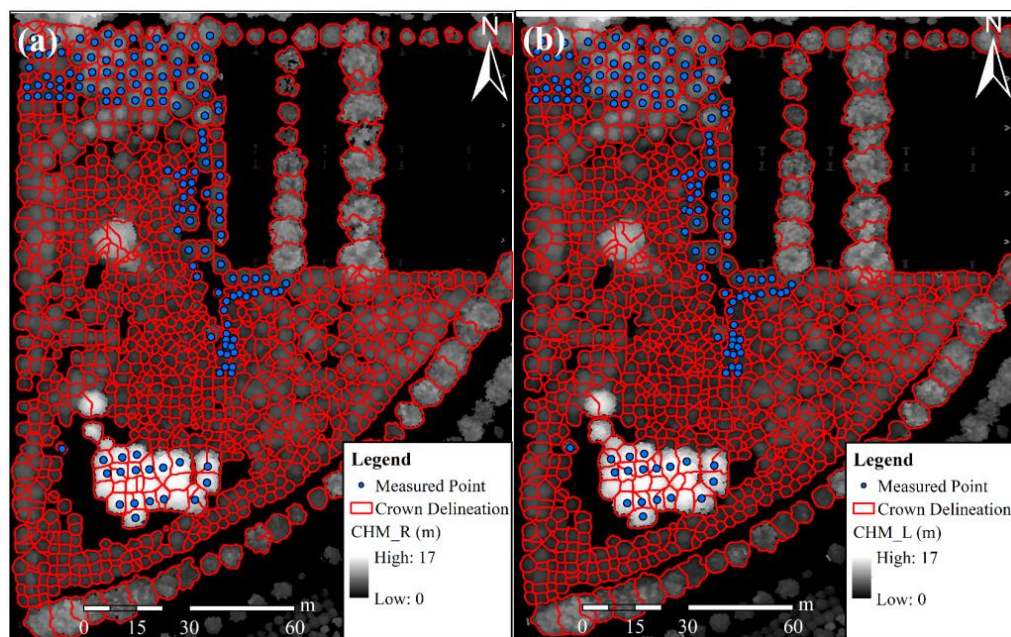


**Figure 8.** Individual tree segmentation results: (a) results based on the CHM generated from image points; (b) results based on the CHM generated from LiDAR points.

**Table 2.** Statistical results of individual tree segmentation. (TP represents the number of trees that are correctly segmented; FN represents the number of trees that are under-segmented; FP represents the number of trees that are over-segmented; r represents recall; p represents precision; F represents F-score).

Data Type	Quantity (Trees)	TP	FN	FP	r (%)	p (%)	F (%)
UAV-RGB	143	118	10	15	92.19	88.72	90.42
UAV-LiDAR	143	112	13	18	89.60	86.15	87.84

Based on Table 2, it is shown that for the segmentation results of the image points, fifteen trees were over-segmented, seven trees were under-segmented, and three trees were not segmented, resulting in an r of 92.19%, p of 88.72%, and F of 90.42%. For the segmentation results of the LiDAR points, eighteen trees were over-segmented, six trees were under-segmented, and seven trees were not segmented, resulting in an r of 89.60%, p of 86.15%, and F of 87.84%. The results indicate that the individual tree segmentation results of the image points are better than those of the LiDAR points.

## 2. Result of Tree Crown Width Extraction

To further quantify the differences in crown width extraction based on image points and LiDAR points, a correlation analysis was conducted between the crown width extraction results and the field-measured crown widths, as shown in Figure 9.

From the results shown in Figure 9, the results of the crown width extraction based on image points and LiDAR points exhibit a high correlation with the field-measured crown widths. Additionally, the crown width extraction results based on the LiDAR points have a higher correlation ( $R^2 = 0.93$ , RMSE = 0.79 m) than those based on the image points ( $R^2 = 0.88$ , RMSE = 0.89 m). Performing a *t*-test to obtain the difference between the crown width extraction results, the *p*-value was 0.19, which is much greater than 0.05, indicating that there is no significant difference in crown width extraction results between the image points and LiDAR points.

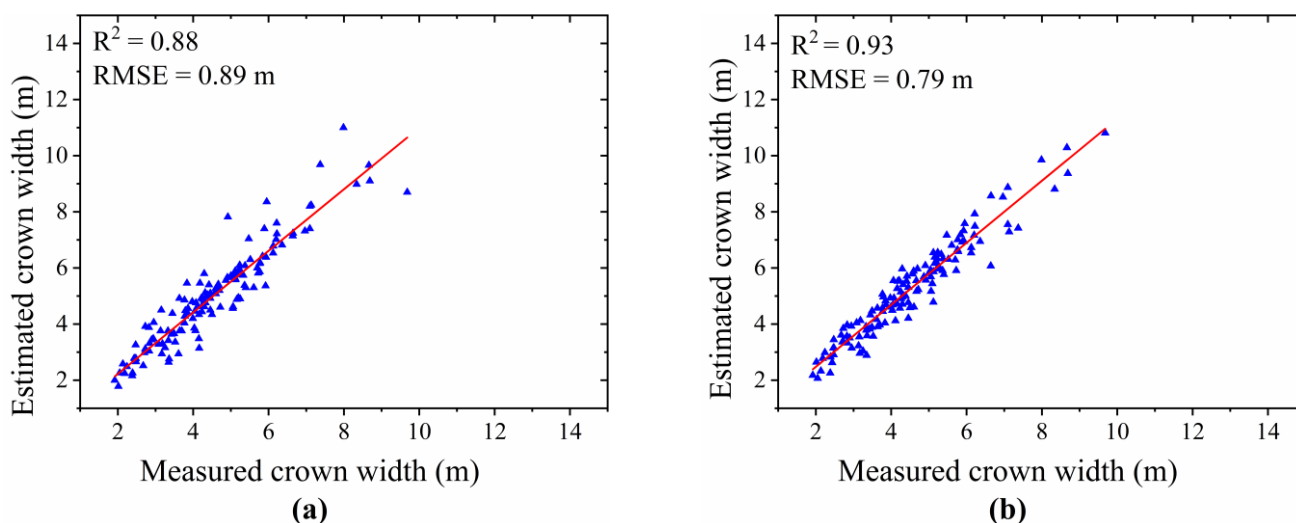


**Figure 9.** Crown width correlation analysis results: (a) correlation between crown width extracted from image points and field-measured crown width; (b) correlation between crown width extracted from LiDAR points and field-measured crown width.

### 3. Result of Tree Height Extraction

Similarly, correlation analysis was conducted between the individual tree height extraction results and the field-measured tree height, as shown in Figure 10.

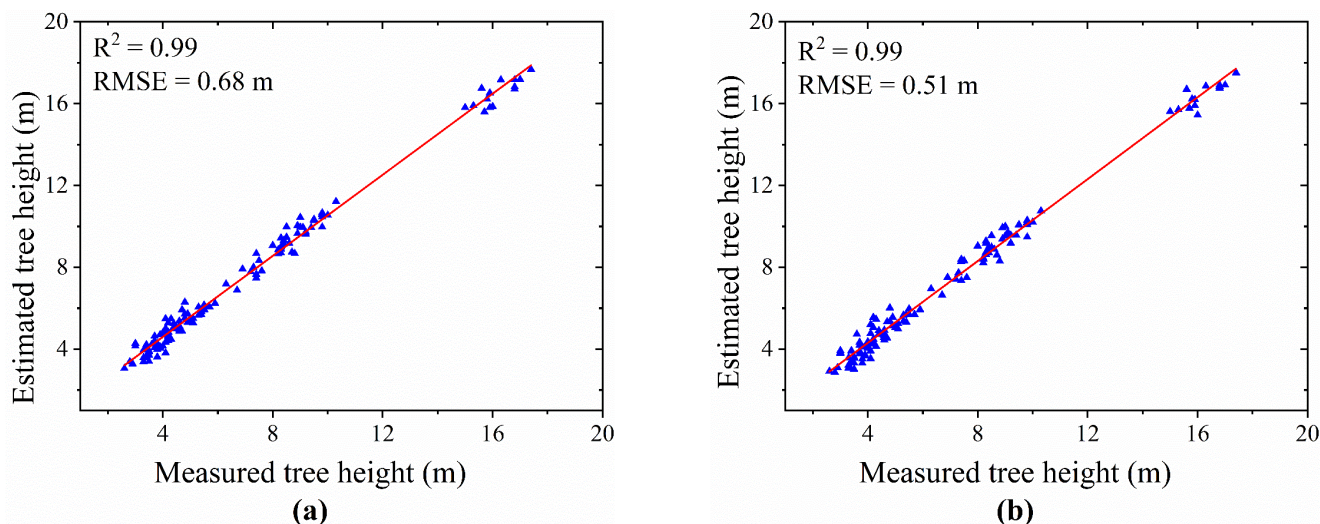


**Figure 10.** Tree height correlation analysis results: (a) correlation between tree height extracted from image points and field-measured tree height; (b) correlation between tree height extracted from LiDAR points and field-measured tree height.

As shown in Figure 10, the extraction results of the tree height based both on image points and LiDAR points exhibit a high correlation with the field-measured tree height, with an  $R^2$  of 0.99 and 0.99, and a RMSE of 0.68 and 0.51 m, respectively. Performing a *t*-test to obtain the difference between tree height extraction results, the *p*-value was 0.60, which is much greater than 0.05, indicating that there is no significant difference in tree height extraction results between the image points and LiDAR points. Therefore, under cost-control conditions, image points can be used to replace LiDAR points for extracting individual tree structural parameters.

### 3.3. Comparison of Crown Width and Height Extraction Results for Different Tree Species

To explore the differences in crown width and tree height extraction results of different tree species based on LiDAR points and image points, four tree species (*Cinnamomum camphora*, *Osmanthus fragrans*, *Liriodendron chinense*, and *Magnolia grandiflora*) were studied.

#### 1. Extraction Results of Crown Width for Different Tree Species

Based on LiDAR points and image points, the crown widths of four tree species were extracted; the correlation results with the field-measured crown widths are shown in Figure 11.

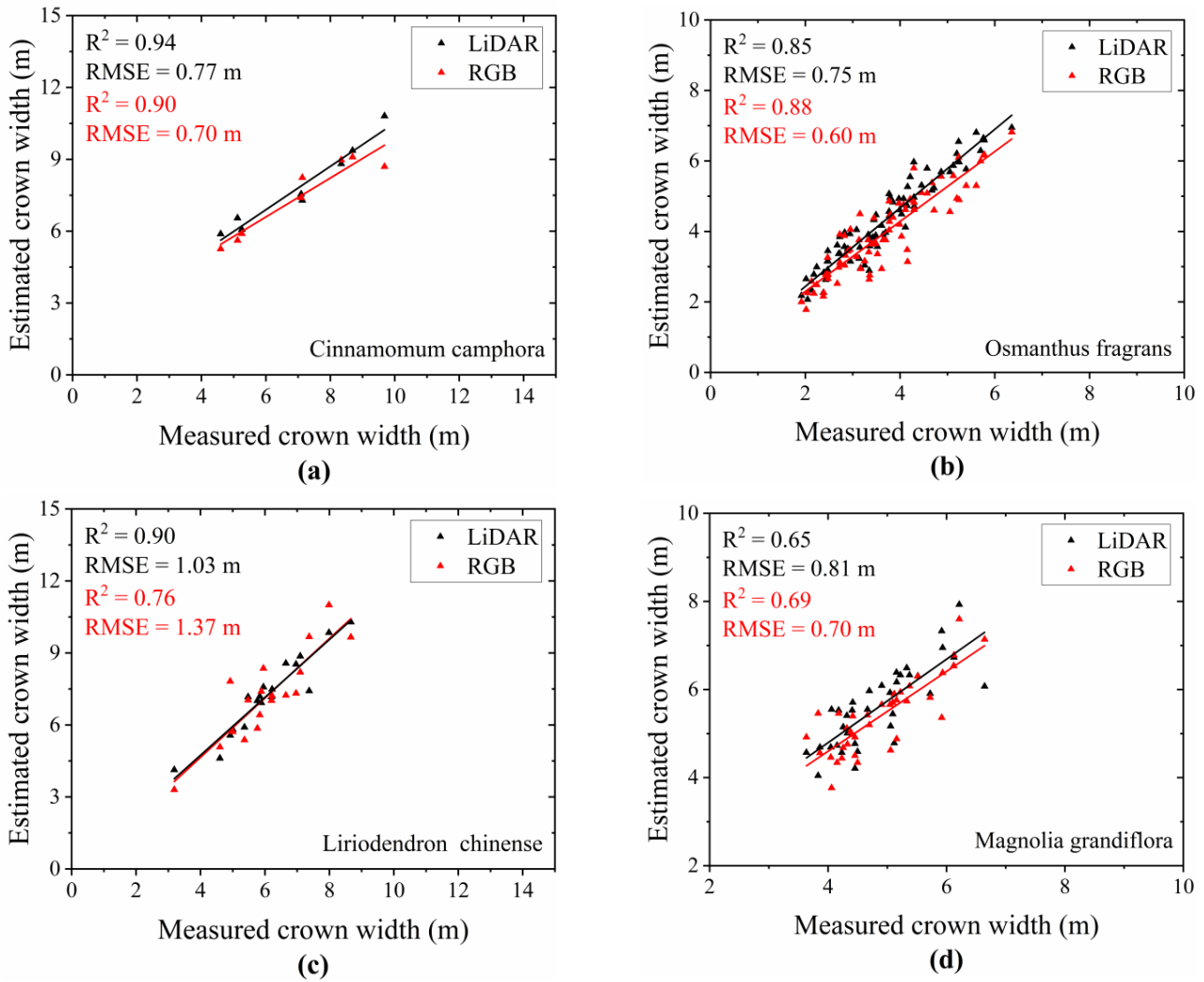


**Figure 11.** Correlation results between field-measured and extracted crown width of different tree species based on LiDAR points and image points: (a) *Cinnamomum camphora*; (b) *Osmanthus fragrans*; (c) *Liriodendron chinense*; (d) *Magnolia grandiflora*.

From the results shown in Figure 11, among four different tree species, the crown width extraction accuracy of *Cinnamomum camphora* is the highest, with an  $R^2$  of 0.94 and a RMSE of 0.77 m for LiDAR points, and with an  $R^2$  of 0.90 and a RMSE of 0.70 m for image points. The crown width extraction accuracy of *Magnolia grandiflora* is the lowest, with an  $R^2$  of 0.65 and a RMSE of 0.81 m for LiDAR points, and with an  $R^2$  of 0.69 and a RMSE of 0.70 m for image points. For *Cinnamomum camphora* and *Liriodendron chinense*, the crown width extraction results based on the LiDAR points are better than those obtained from the image points. However, for *Osmanthus fragrans* and *Magnolia grandiflora*, the crown width extraction results based on the image points are superior to those obtained

from the LiDAR points. In the case of *Liriodendron chinense*, the difference in crown extraction results between the LiDAR points and image points is the greatest, with an  $R^2$  of 0.90 and a RMSE of 1.03 m for the LiDAR points, and with an  $R^2$  of 0.76 and a RMSE of 1.37 m for the image points. The  $R^2$  and RMSE were 0.14 and 0.34 m, respectively. For the remaining three tree species, the differences in the crown extraction results between the LiDAR points and image points are relatively small, with the maximum difference of 0.04 for the  $R^2$  and 0.15 m for the RMSE.

To further test whether the differences in the crown width extraction results are significant, one-way analysis of variance (ANOVA) was performed on the crown width extraction results of four tree species based on LiDAR points and image points using Origin Pro 2018 software, as shown in Tables 3 and 4.

**Table 3.** Analysis of variance for crown width of different tree species extracted from both LiDAR points and image points.

-	Data Sources	DF	Square Sum	Mean Square	F	p
Model		3	193.43	64.48	41.03	0
Error	LiDAR points	140	207.41	1.57	-	-
Total		143	400.84	-	-	-
Model		3	219.28	73.09	48.75	0
Error	Image points	140	197.71	1.50	-	-
Total		143	417.18	-	-	-

Note: DF represents the degrees of freedom.

**Table 4.** Tukey's test for crown width extraction results of different tree species based on LiDAR points and image points.

Data Sources	Species	Mean Square	SEM	q	p	Alpha	Sig
LiDAR points	a and b	3.49	0.47	10.58	0	0.05	1
	a and c	1.56	0.53	1.50	0	0.05	1
	a and d	2.17	0.49	6.27	0	0.05	1
	b and c	2.93	0.33	12.56	0	0.05	1
	b and d	1.33	0.25	7.42	0	0.05	1
	c and d	-1.60	0.36	6.29	0	0.05	1
	a and b	3.45	0.46	10.69	0	0.05	1
Image points	a and c	1.59	0.52	0.53	0	0.05	1
	a and d	2.00	0.48	5.94	0	0.05	1
	b and c	3.25	0.32	14.27	0	0.05	1
	b and d	1.44	0.25	8.25	0	0.05	1
	c and d	-1.81	0.35	7.28	0	0.05	1

Note: a, b, c, and d represent *Cinnamomum camphora*, *Osmanthus fragrans*, *Liriodendron chinense*, and *Magnolia grandiflora*, respectively. SEM (standard error of the mean) represents the standard error between the sample mean and the population mean; q is used to calculate the mean differences between each treatment group; p represents the probability value; Alpha represents the significance level in Tukey's test; and sig represents the significance level of the test results.

By analyzing the results shown in Table 3, it was found that the  $p$ -values were all less than 0.05, indicating that further Tukey's tests could be performed to analyze the differences in crown width extraction among different tree species. By analyzing the results of Tukey's tests on the differences in crown width extraction among different tree species shown in Table 4, it was found that all the  $p$ -values were less than 0.05, indicating that all the differences in crown width extraction results among different tree species based on both LiDAR points and image points were significant.

## 2. Extraction Results of Tree Height for Different Tree Species

Similarly, the correlation results between the field-measured and the extracted tree heights of different tree species based on LiDAR points and image points are shown in Figure 12.

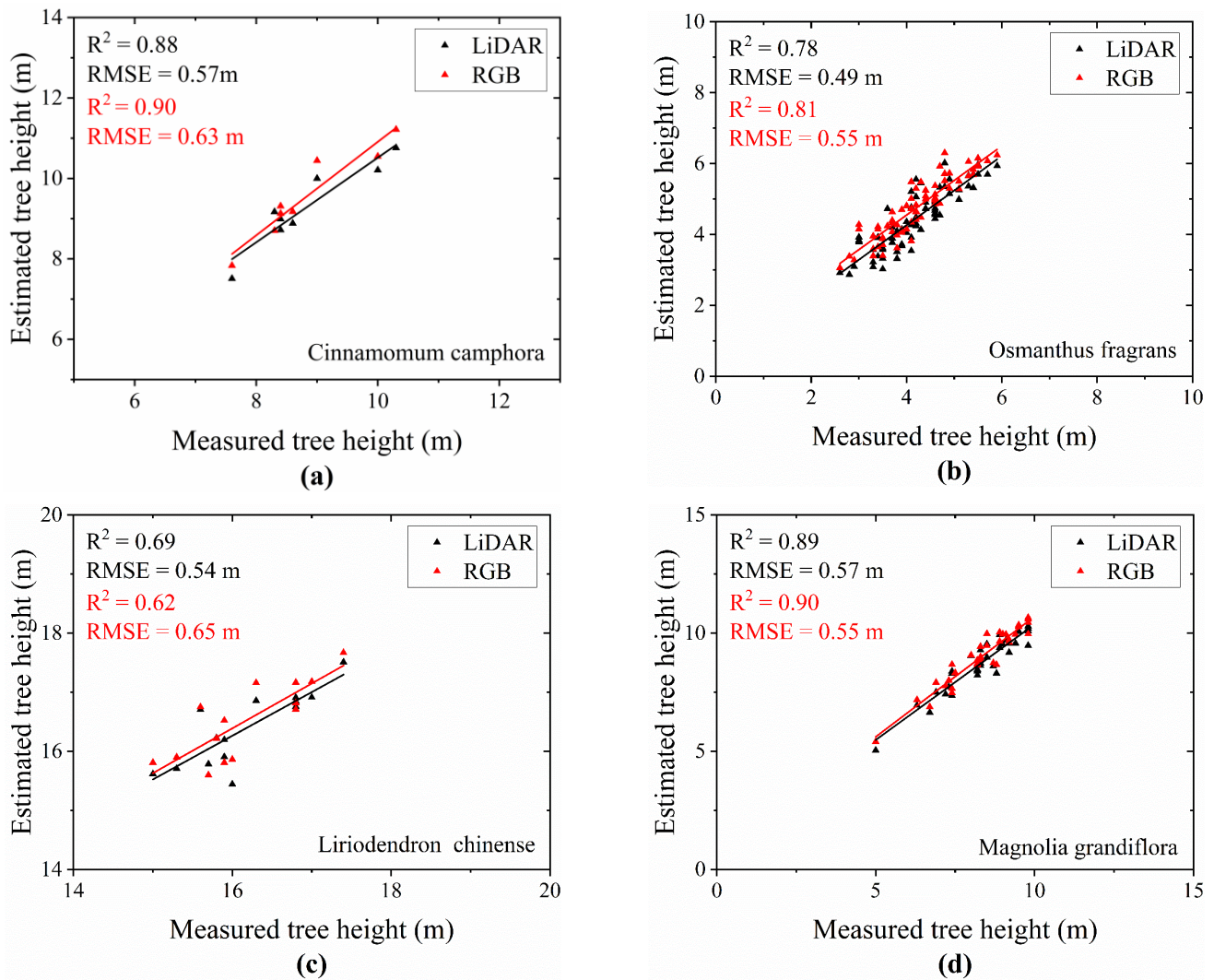


**Figure 12.** Correlation results between the measured tree heights and the extracted tree heights of different tree species based on LiDAR points and image points: (a) *Cinnamomum camphora*; (b) *Osmanthus fragrans*; (c) *Liriodendron chinense*; (d) *Magnolia grandiflora*.

The results presented in Figure 12 suggest that among four different tree species, the tree height extraction accuracy of *Magnolia grandiflora* is the highest, with an R<sup>2</sup> of 0.89 and a RMSE of 0.57 m for LiDAR points, and with an R<sup>2</sup> of 0.90 and a RMSE of 0.62 m for image points. In contrast, the tree height extraction accuracy of *Liriodendron chinense* is the lowest, with an R<sup>2</sup> of 0.69 and a RMSE of 0.54 m for LiDAR points, and with an R<sup>2</sup> of 0.62 and a RMSE of 0.65 m for image points. For *Liriodendron chinense*, the tree height extraction results based on LiDAR points outperform those obtained from image points. In contrast, for *Cinnamomum camphora*, *Osmanthus fragrans*, and *Magnolia grandiflora*, the tree height extraction results based on image points are superior to those obtained from LiDAR points. Specifically, the difference in tree height extraction results between the LiDAR points and image points is the largest for *Liriodendron chinense*, with a difference in R<sup>2</sup> of 0.07 and in RMSE of 0.11 m. Comparatively, for the other three tree species, the differences in R<sup>2</sup> and RMSE are relatively small, with the maximum differences in R<sup>2</sup> and RMSE being 0.03 and 0.06 m, respectively.

To further test whether the differences in tree height extraction results are significant, Origin Pro 2018 software was used to perform ANOVA, and the results are shown in Tables 5 and 6.

**Table 5.** Analysis of variance for tree heights of different tree species extracted from both LiDAR points and image points.

-	Data Sources	DF	Square Sum	Mean Square	F	p
Model		3	1807.52	602.51	674.85	0
Error	LiDAR points	140	107.14	0.89	-	-
Total		143	1914.66	-	-	-
Model		3	1766.07	588.69	649.71	0
Error	Image points	140	108.73	0.91	-	-
Total		143	1874.80	-	-	-

**Table 6.** Tukey's test for tree height extraction results of different tree species based on LiDAR points and image points.

Data Sources	Species	Mean Square	SEM	q	p	Alpha	Sig
LiDAR points	a and b	4.83	0.35	19.32	0	0.05	1
	a and c	-7.10	0.42	23.99	0	0.05	1
	a and d	3.54	0.37	12.07	0	0.05	1
	b and c	11.93	0.28	60.84	0	0.05	1
	b and d	44.28	0.20	30.51	0	0.05	1
	c and d	-7.65	0.30	36.05	0	0.05	1
Image points	a and b	4.80	0.36	19.11	0	0.05	1
	a and c	-6.97	0.42	23.36	0	0.05	1
	a and d	3.71	0.37	12.13	0	0.05	1
	b and c	11.78	0.28	59.61	0	0.05	1
	b and d	4.26	0.20	30.16	0	0.05	1
	c and d	-7.51	0.30	35.15	0	0.05	1

Note: a, b, c, and d represent *Cinnamomum camphora*, *Osmanthus fragrans*, *Liriodendron chinense*, and *Magnolia grandiflora*, respectively. SEM (standard error of the mean) represents the standard error between the sample mean and the population mean; q is used to calculate the mean differences between each treatment group; p represents the probability value; Alpha represents the significance level in Tukey's test; and sig represents the significance level of the test results.

By analyzing the results shown in Table 5, it was found that all the *p*-values were less than 0.05, indicating that further Tukey's tests could be performed to analyze the differences in tree height extraction among different tree species. By analyzing the results of the Tukey's tests shown in Table 6, it was found that all the *p*-values were less than 0.05, indicating that all the differences in tree height extraction results among different tree species based on both LiDAR points and image points were significant.

To summarize, for the extraction of the individual tree crown width and tree height, the results of different tree species based on LiDAR points and image points are different. Statistics are provided on the methods with better extraction results for individual tree crown width and tree height of different tree species, as shown in Table 7.

**Table 7.** Statistics on methods with greater extraction results for individual tree crown width and tree height of different tree species.

Tree Species/ Structural Parameters	Crown Width	Tree Height
<i>Cinnamomum camphora</i>	UAV-LiDAR	UAV-RGB
<i>Osmanthus fragrans</i>	UAV-RGB	UAV-RGB
<i>Liriodendron chinense</i>	UAV-LiDAR	UAV-LiDAR
<i>Magnolia grandiflora</i>	UAV-RGB	UAV-RGB

As shown in Table 7, for the extraction of individual tree structural parameters, the LiDAR points and image points have their own advantages and disadvantages, and the extraction accuracy is closely related to the tree species.

## 4. Discussion

### 4.1. Differences in Analysis of DEM and DSM Results

In this study, LiDAR points and image points were used to generate DEMs. The results showed that the DEM generated based on LiDAR points had greater accuracy than that obtained from image points, but the difference was not significant. This finding is in line with the results of previous studies. For instance, Tilly et al. [28] studied the difference between the DEMs generated from UAV image points and LiDAR points, and the results showed that the accuracy of the DEM generated from the LiDAR points was greater than that obtained from the image points. Wilkinson et al. [29] conducted a similar study and obtained the same conclusion. The difference is closely related to the principles of obtaining 3D point data for LiDAR points and image points; that is, LiDAR points obtain 3D point data through obtaining laser pulse echoes, while image points generate 3D point data through stereo image calculation. Thus, LiDAR can penetrate the forest canopy and obtain more ground points, whereas image points mainly consist of many canopy points and a few ground points under the canopy. For example, the differences between the DEMs in cross sections a and b indicate that in areas without trees, the elevation values of the two DEMs are almost identical. In areas with a forest canopy, the DEM generated based on the LiDAR points is more accurate than that obtained from the image points. Furthermore, as the forest canopy closure increases, the difference between the elevation values of the two DEMs tends to increase. This is similar to previous research findings, such as the research of Guerra-Hernández et al. [16], who found that the terrain surface elevation generated based on UAV images was slightly higher than that generated by LiDAR, with an average difference of 1.14 m and a standard deviation of 1.93 m. Goodbody et al. [30] investigated the effect of forest canopy closure on DEMs by employing UAV images and UAV-LiDAR, and found that for every 10% in the forest canopy closure, the error of the DEM increased by approximately 0.03 m. In addition to the forest canopy closure, the ground slope is also a major factor that affects the generation of DEMs from ground points. For flat terrain, even if the high forest canopy closure results in less ground points being obtained, a relatively accurate DEM can still be obtained through interpolation algorithms. However, when the topography beneath the forest is rugged and the slope is steep, the accuracy of DEM interpolation is to some extent compromised [31]. Therefore, in future research on forest structural parameter estimation using the DEM, when the forest canopy closure is relatively low or the terrain is relatively flat, UAV-LiDAR or UAV-RGB images can be used for direct measurement. However, in forest stands with relatively high canopy closure and a complex terrain, it is recommended to frequently use high-precision positioning equipment such as total stations to obtain ground points under the canopy to generate more accurate DEMs, as well as to further improve the accuracy of forest structural parameter estimation.

In addition to the DEM, the DSM is also a key factor affecting the quality of the CHM and thus plays an important role in the extraction of individual tree structural parameters. In this study, both LiDAR points and image points were used to generate DSMs, and the DSMs generated from LiDAR points always had higher elevation values than those generated from image points in grassland or forest areas (as shown in Figures 6 and 7). This was mainly due to the randomness and discreteness of LiDAR points; it is not possible to accurately locate key positions in the vegetation canopy, such as the crown vertex. Therefore, it is difficult to accurately obtain crown vertex information from LiDAR points. The maximum value obtained based on LiDAR points may come from the area near the crown vertex rather than the actual tree vertex, commonly resulting in the extracted tree height being lower than the actual value. In addition, LiDAR points can penetrate the surface of the vegetation within the interior of the canopy and even the ground. In contrast, the image points were obtained from stereo images using the SFM algorithm, which can more easily obtain key positions on the surface of vegetation canopy in unobstructed areas, such as the crown vertex. Based on the above reasons, the estimated elevation values of the image points were relatively higher than those obtained from the LiDAR points in grassland and forest areas. However, in non-vegetation areas, the elevation values estimated by the



LiDAR points and image points were basically the same. This is also the reason why the tree heights extracted from image points are relatively higher than those extracted from LiDAR points (as shown in Figure 12). The results indicate that there were relatively large differences between the DSMs generated from the two types of data in the vegetation areas, whereas the differences were relatively minor in the non-vegetation areas. This finding is consistent with the results of earlier research, such as that conducted by Rogers et al. [32], who studied the differences between DSMs generated from UAV photogrammetry and LiDAR data, and found that the differences were relatively large in the vegetation area, while the differences were small in the non-vegetation area.

#### 4.2. Analyzing the Differences between the Extraction Results of the Structural Parameters of Individual Trees

As the main forms of acquiring 3D point data, LiDAR points and image points are widely used in the extraction of individual tree structural parameters. For example, Zarco-Tejada et al. [33] estimated the individual tree height of an olive tree through a UAV equipped with an RGB camera, and the results demonstrated an  $R^2$  of 0.93 and a RMSE of 0.35 m. Yu et al. [34] used multi-temporal UAV LiDAR data to monitor the growth and changes in Scottish pine, resulting in an  $R^2$  of 0.68 and a RMSE of 0.43 m. The above research results indicate that both image points and LiDAR points are indeed capable of accurately extracting an individual tree height. The conclusion of this study is consistent with previous research. In this study, both image points and LiDAR points were used to extract individual tree heights, with an  $R^2$  of 0.99 and 0.99, and a RMSE of 0.68 m and 0.51 m being obtained, respectively. The greater accuracy in obtaining the tree height is mainly related to plantations with a relatively flat terrain and simple structure. Additionally, the results show that there is no significant difference between the tree height extraction results based on the LiDAR points and image points. This is mainly because of the relatively flat terrain and relatively low forest canopy closure in the plantation. Moreover, with the rapid development of the SFM algorithm and computer science, the accuracy of tree height extraction using image points for a plantation is comparable to that obtained from LiDAR points.

In addition to tree height, the crown width of individual trees is also an important structural parameter for volume estimation. In this study, image points and LiDAR points were used to extract the crown width of individual trees, and the result based on the LiDAR points had a higher accuracy ( $R^2 = 0.93$ , RMSE = 0.79 m) than that obtained from the image points ( $R^2 = 0.88$ , RMSE = 0.89 m). By performing a *t*-test, it was demonstrated that there was no significant difference in the crown width extraction results between the image points and LiDAR points. Therefore, under cost-control conditions, image points are able to replace LiDAR points for extracting individual tree structural parameters.

#### 4.3. Analyzing the Differences between the Results of Structural Parameter Extraction for Different Tree Species

The extraction results for the individual tree structural parameters are not only influenced by the data type used, but also by the tree species. The structural characteristics of different tree species differ, and the principles of the acquisition of LiDAR points and image points also differ, resulting in differences in the extraction of structural parameters. As shown in Figure 11, for *Cinnamomum camphora*, *Osmanthus fragrans*, and *Magnolia grandiflora*, the differences in the crown extraction results between the LiDAR points and image points are relatively small, with a maximum difference of 0.04 for the  $R^2$  and 0.15 m for the RMSE. In contrast, for *Liriodendron chinense*, the difference is the greatest, with an  $R^2$  difference of 0.14 and a RMSE difference of 0.34 m. This is mainly determined by the structural differences of different tree species. Specifically, *Cinnamomum camphora*, *Osmanthus fragrans*, and *Magnolia grandiflora* are evergreen trees with umbrella-shaped crowns, while *Liriodendron chinense* are deciduous trees with conical crowns. The conical tree crown and larger crown thickness (the distance from the height of the lowest branch to the crown vertex) usually causes the middle and lower parts of the crown to be obstructed

by adjacent crowns, resulting in the inability to capture unobstructed images of the middle and lower part of the crown from all angles during oblique photography. Therefore, when using the SFM algorithm to generate 3D point cloud data based on obtained stereo images, it is not possible to obtain the complete point cloud data for the middle and lower parts of the tree crown, with the result that the CHM generated based on 3D point cloud data is not able to describe the complete tree crown, ultimately resulting in certain errors in the crown width extraction of individual trees. In contrast, LiDAR obtains point cloud data by emitting laser pulses, which can obtain relatively complete information about the middle and lower canopy parts, thereby achieving accurate extraction of individual tree canopy width. Different crown shapes are the main reason for the differences in crown extraction results between LiDAR points and image points. Thus, in the future, in the case of extracting the crown width of tree species with umbrella-shaped crowns or dense crowns, it is recommended to use the UAV high-resolution image acquisition method. When extracting the crown width of tree species with conical or sparse crowns, the UAV LiDAR method is recommended. However, if the cost needs to be controlled, the UAV high-resolution image method is the optimal choice.

Similarly, the tree heights of four different tree species were extracted separately based on the LiDAR points and image points. The results showed that for *Liriodendron chinense*, the tree height extraction results based on the LiDAR points were better than those derived from the image points. For *Cinnamomum camphora*, *Osmanthus fragrans*, and *Magnolia grandiflora*, the tree height extraction results based on the image points were superior to those obtained from the LiDAR points. Although for different tree species there are differences in the tree height extraction results between the LiDAR points and image points, the differences are relatively small, with a maximum  $R^2$  difference of 0.07 and a maximum RMSE difference of 0.11 m. The results indicate that there is little difference in the results between the LiDAR points and image points when extracting the height of the same tree species. When the heights of different tree species were extracted, the accuracy of determining the tree height of *Liriodendron chinense* was the lowest among the four tree species. This is mainly because the crown of *Liriodendron chinense* has a conical structure, and both LiDAR points and image points cannot capture the crown vertex well, resulting in relatively weak tree height extraction results. Therefore, in future research on estimating the height of individual trees, the UAV high-resolution image method is recommended, which can greatly save on costs while still ensuring accuracy.

As shown in Table 1, the standard deviations of the tree height and crown width for each tree species in the study area are relatively small; thus, the above results were obtained. However, when the forest trees have more variability in tree height, crown width, and forest age, the results of tree height and crown width extraction, as well as the differences in extraction results among different tree species may be different from the results of our study area.

## 5. Conclusions

The results of this study indicate that both LiDAR points and image points can generate accurate DEMs and DSMs and accurately extract individual tree height and crown width. This not only provides economically reliable technical means for the monitoring of forest time-series growth, but also provides basic data for a global correction of understory DEMs through the generation of high-accuracy DEMs. At the same time, accurate extraction of individual tree structural parameters can not only provide high-precision verification data for other data sources, such as ICESAT-2 and GF-7, but also provide data support for other related research, such as on carbon storage estimation, biodiversity, climate change, digital city modeling, etc. However, there are still some limitations in the study. In particular, the terrain of the study area is relatively flat, with little variation in slope and relatively simple plantation forest structures. In addition, when extracting and comparing the differences in individual tree structural parameters of different tree species using two forms of data, only the differences between four different broad-leaved tree species were considered, without

considering the differences between more tree species or coniferous tree species. Therefore, in future studies, more complex terrain and more diverse tree species should be considered to further validate the differences between extracting individual structural parameters with LiDAR points and image points.

**Author Contributions:** Conceptualization, H.Y. and F.W.; data curation, H.Y., X.T. and Q.Y.; formal analysis, H.Y. and X.T.; methodology, X.T., H.Y. and F.W.; supervision, Y.L. and J.C.; validation, F.W.; writing—original draft preparation, H.Y., X.T. and Q.Y.; writing—review and editing, X.T. and H.Y. All authors have read and agreed to the published version of the manuscript.

**Funding:** This study was supported by grants from the National Natural Science Foundation of China (42261063, 41901370), Guangxi Natural Science Foundation (2020GXNSFBA297096), Guangxi Science and Technology Base and Talent Project (GuikeAD19245032), and the BaGuiScholars program of the provincial government of Guangxi (Hongchang He).

**Institutional Review Board Statement:** Not applicable.

**Informed Consent Statement:** Not applicable.

**Data Availability Statement:** Not applicable.

**Conflicts of Interest:** The authors declare no conflict of interest.

## References

- Dandois, J.P.; Olano, M.; Ellis, E.C. Optimal altitude, overlap, and weather conditions for computer vision UAV estimates of forest structure. *Remote Sens.* **2015**, *7*, 13895–13920. [[CrossRef](#)]
- Clark, M.L.; Clark, D.B.; Roberts, D.A. Small-footprint lidar estimation of sub-canopy elevation and tree height in a tropical rain forest landscape. *Remote Sens. Environ.* **2004**, *91*, 68–89. [[CrossRef](#)]
- Maltamo, M.; Peuhkurinen, J.; Malinen, J.; Vauhkonen, J.; Packalén, P.; Tokola, T. Predicting tree attributes and quality characteristics of Scots pine using airborne laser scanning data. *Silva Fenn.* **2009**, *43*, 507–521. [[CrossRef](#)]
- Latifi, H.; Fassnacht, F.; Koch, B. Forest structure modeling with combined airborne hyperspectral and LiDAR data. *Remote Sens. Environ.* **2012**, *121*, 10–25. [[CrossRef](#)]
- Hudak, A.T.; Crookston, N.L.; Evans, J.S.; Falkowski, M.J.; Smith, A.M.; Gessler, P.E.; Morgan, P. Regression modeling and mapping of coniferous forest basal area and tree density from discrete-return lidar and multispectral satellite data. *Can. J. Remote Sens.* **2006**, *32*, 126–138. [[CrossRef](#)]
- Jaakkola, A.; Hyyppä, J.; Kukko, A.; Yu, X.; Kaartinen, H.; Lehtomäki, M.; Lin, Y. A low-cost multi-sensoral mobile mapping system and its feasibility for tree measurements. *ISPRS J. Photogramm. Remote Sens.* **2010**, *65*, 514–522. [[CrossRef](#)]
- da Cunha Neto, E.M.; Rex, F.E.; Veras, H.F.P.; Moura, M.M.; Sanquetta, C.R.; Käfer, P.S.; Sanquetta, M.N.I.; Zambrano, A.M.A.; Broadbent, E.N.; Dalla Corte, A.P. Using high-density UAV-Lidar for deriving tree height of *Araucaria Angustifolia* in an Urban Atlantic Rain Forest. *Urban For. Urban Green.* **2021**, *63*, 127197. [[CrossRef](#)]
- Iglhaut, J.; Cabo, C.; Puliti, S.; Piermattei, L.; O'Connor, J.; Rosette, J. Structure from motion photogrammetry in forestry: A review. *Curr. For. Rep.* **2019**, *5*, 155–168. [[CrossRef](#)]
- Chen, J.; Chen, Z.; Huang, R.; You, H.; Han, X.; Yue, T.; Zhou, G. The Effects of Spatial Resolution and Resampling on the Classification Accuracy of Wetland Vegetation Species and Ground Objects: A Study Based on High Spatial Resolution UAV Images. *Drones* **2023**, *7*, 61. [[CrossRef](#)]
- Thiel, C.; Schmullius, C. Comparison of UAV photograph-based and airborne lidar-based point clouds over forest from a forestry application perspective. *Int. J. Remote Sens.* **2017**, *38*, 2411–2426. [[CrossRef](#)]
- Torresan, C.; Berton, A.; Carotenuto, F.; Di Gennaro, S.F.; Gioli, B.; Matese, A.; Miglietta, F.; Vagnoli, C.; Zaldei, A.; Wallace, L. Forestry applications of UAVs in Europe: A review. *Int. J. Remote Sens.* **2017**, *38*, 2427–2447. [[CrossRef](#)]
- Karpina, M.; Jarzabek-Rychard, M.; Tymków, P.; Borkowski, A. UAV-based automatic tree growth measurement for biomass estimation. *Int. Arch. Photogramm. Remote Sens. Spat. Inf. Sci.* **2016**, *8*, 685–688. [[CrossRef](#)]
- Guerra-Hernández, J.; González-Ferreiro, E.; Monleón, V.J.; Faias, S.P.; Tomé, M.; Díaz-Varela, R.A. Use of multi-temporal UAV-derived imagery for estimating individual tree growth in *Pinus pinea* stands. *Forests* **2017**, *8*, 300. [[CrossRef](#)]
- Tang, X.; You, H.; Liu, Y.; You, Q.; Chen, J. Monitoring of Monthly Height Growth of Individual Trees in a Subtropical Mixed Plantation Using UAV Data. *Remote Sens.* **2023**, *15*, 326. [[CrossRef](#)]
- Dempewolf, J.; Nagol, J.; Hein, S.; Thiel, C.; Zimmermann, R. Measurement of within-season tree height growth in a mixed forest stand using UAV imagery. *Forests* **2017**, *8*, 231. [[CrossRef](#)]
- Guerra-Hernández, J.; Cosenza, D.N.; Rodriguez, L.C.E.; Silva, M.; Tomé, M.; Díaz-Varela, R.A.; González-Ferreiro, E. Comparison of ALS-and UAV (SfM)-derived high-density point clouds for individual tree detection in *Eucalyptus* plantations. *Int. J. Remote Sens.* **2018**, *39*, 5211–5235. [[CrossRef](#)]

17. Wallace, L.; Lucieer, A.; Malenovský, Z.; Turner, D.; Vopěnka, P. Assessment of forest structure using two UAV techniques: A comparison of airborne laser scanning and structure from motion (SfM) point clouds. *Forests* **2016**, *7*, 62. [[CrossRef](#)]
18. Guerra-Hernández, J.; Cosenza, D.N.; Cardil, A.; Silva, C.A.; Botequim, B.; Soares, P.; Silva, M.; González-Ferreiro, E.; Díaz-Varela, R.A. Predicting growing stock volume of eucalyptus plantations using 3-D point clouds derived from UAV imagery and ALS data. *Forests* **2019**, *10*, 905. [[CrossRef](#)]
19. Khosravipour, A.; Skidmore, A.K.; Isenburg, M.; Wang, T.; Hussin, Y.A. Generating Pit-free Canopy Height Models from Airborne Lidar. *Photogramm. Eng. Remote Sens.* **2014**, *80*, 863–872. [[CrossRef](#)]
20. Zhao, X.; Guo, Q.; Su, Y.; Xue, B. Improved progressive TIN densification filtering algorithm for airborne LiDAR data in forested areas. *ISPRS J. Photogramm. Remote Sens.* **2016**, *117*, 79–91. [[CrossRef](#)]
21. Tanhuanpää, T.; Saarinen, N.; Kankare, V.; Nurminen, K.; Vastaranta, M.; Honkavaara, E.; Karjalainen, M.; Yu, X.; Holopainen, M.; Hyyppä, J. Evaluating the Performance of High-Altitude Aerial Image-Based Digital Surface Models in Detecting Individual Tree Crowns in Mature Boreal Forests. *Forests* **2016**, *7*, 143. [[CrossRef](#)]
22. Chen, Q.; Baldocchi, D.; Gong, P.; Kelly, M. Isolating individual trees in a savanna woodland using small footprint lidar data. *Photogramm. Eng. Remote Sens.* **2006**, *72*, 923–932. [[CrossRef](#)]
23. Miraki, M.; Sohrabi, H.; Fatehi, P.; Kneubuehler, M. Individual tree crown delineation from high-resolution UAV images in broadleaf forest. *Ecol. Inform.* **2021**, *61*, 101207. [[CrossRef](#)]
24. Nuijten, R.J.; Coops, N.C.; Goodbody, T.R.; Pelletier, G. Examining the multi-seasonal consistency of individual tree segmentation on deciduous stands using digital aerial photogrammetry (DAP) and unmanned aerial systems (UAS). *Remote Sens.* **2019**, *11*, 739. [[CrossRef](#)]
25. Panagiotidis, D.; Abdollahnejad, A.; Surový, P.; Chiteculo, V. Determining tree height and crown diameter from high-resolution UAV imagery. *Int. J. Remote Sens.* **2017**, *38*, 2392–2410. [[CrossRef](#)]
26. Goldbergs, G.; Maier, S.W.; Levick, S.R.; Edwards, A. Efficiency of individual tree detection approaches based on light-weight and low-cost UAS imagery in Australian Savannas. *Remote Sens.* **2018**, *10*, 161. [[CrossRef](#)]
27. Yin, D.; Wang, L. How to assess the accuracy of the individual tree-based forest inventory derived from remotely sensed data: A review. *Int. J. Remote Sens.* **2016**, *37*, 4521–4553. [[CrossRef](#)]
28. Tilly, N.; Kelterbaum, D.; Zeese, R. Geomorphological Mapping With Terrestrial Laser Scanning And Uav-Based Imaging. *Int. Arch. Photogramm. Remote Sens. Spat. Inf. Sci.* **2016**, *41*, 591–597. [[CrossRef](#)]
29. Wilkinson, M.; Jones, R.; Woods, C.; Gilment, S.; McCaffrey, K.; Kokkalas, S.; Long, J. A comparison of terrestrial laser scanning and structure-from-motion photogrammetry as methods for digital outcrop acquisition. *Geosphere* **2016**, *12*, 1865–1880. [[CrossRef](#)]
30. Goodbody, T.R.H.; Coops, N.C.; Hermosilla, T.; Tompalski, P.; Pelletier, G. Vegetation Phenology Driving Error Variation in Digital Aerial Photogrammetrically Derived Terrain Models. *Remote Sens.* **2018**, *10*, 1554. [[CrossRef](#)]
31. Nikolakopoulos, K.G.; Antonakakis, A.; Kyriou, A.; Koukouvelas, I.; Stefanopoulos, P. Comparison of terrestrial laser scanning and structure-from-motion photogrammetry for steep slope mapping. In Proceedings of the Earth Resources and Environmental Remote Sensing/GIS Applications IX, Berlin, Germany, 11–13 September 2018; pp. 95–105.
32. Rogers, S.R.; Manning, I.; Livingstone, W. Comparing the Spatial Accuracy of Digital Surface Models from Four Unoccupied Aerial Systems: Photogrammetry Versus LiDAR. *Remote Sens.* **2020**, *12*, 2806. [[CrossRef](#)]
33. Zarco-Tejada, P.J.; Diaz-Varela, R.; Angileri, V.; Loudjani, P. Tree height quantification using very high resolution imagery acquired from an unmanned aerial vehicle (UAV) and automatic 3D photo-reconstruction methods. *Eur. J. Agron.* **2014**, *55*, 89–99. [[CrossRef](#)]
34. Yu, X.; Hyyppä, J.; Kukko, A.; Maltamo, M.; Kaartinen, H. Change detection techniques for canopy height growth measurements using airborne laser scanner data. *Photogramm. Eng. Remote Sens.* **2006**, *72*, 1339–1348. [[CrossRef](#)]

**Disclaimer/Publisher’s Note:** The statements, opinions and data contained in all publications are solely those of the individual author(s) and contributor(s) and not of MDPI and/or the editor(s). MDPI and/or the editor(s) disclaim responsibility for any injury to people or property resulting from any ideas, methods, instructions or products referred to in the content.